ACADEMIA ROMÂNĂ
Revue Roumaine de Chimie
http://web.icf.ro/rrch/

Rev. Roum. Chim.,
2011, *56*(10-11), 947-952

SYNTHESIS OF MESOPOROUS CARBON MATERIALS *via* NANOCASTING ROUTE – COMPARATIVE STUDY OF GLYCEROL AND SUCROSE AS CARBON SOURCES

Maria IGNAT* and Evelini POPOVICI

Laboratory of Materials Science, Department of Chemistry, Faculty of Chemistry, "Al. I. Cuza" University of Iaşi, 11 Carol I Bvd., Iaşi 700506, Roumania

Received June 2, 2010

In this work, mesoporous carbon has been synthesized using mesoporous silica molecular sieves as templates. Using highly ordered mesoporous silica as template, nanocasting has brought forward incredible possibilities in preparing novel mesostructured materials. The mesoporous silica allows controlling the pore diameters, providing new possibilities for many applications in adsorption and catalysis. In a synthesis process of mesoporous carbon materials *via* nanocasting route, different types of carbon precursors could be used. Firstly, the infiltrated carbon precursor into silica mesopores is subjected to a polymerization process, and then carbonized in order to obtain the carbon framework. The silica template is subsequently removed with hydrofluoric acid and the mesoporous carbon is successfully obtained. Taking into account that the nature of the carbon precursor may influence some of the carbons characteristics, next we will present a comparative study of sucrose-based and glycerol-based mesoporous carbons templated on SBA-15 mesoporous silica. N_2 sorption, XRD, TGA and SEM were used to characterize the synthesized carbon materials.

INTRODUCTION

Nanostructured materials have attracted a large interest for various applications such as storage of hydrogen and methane, supercapacitor, molecular separation, adsorption and catalysis.[1-3] Nanocasting is a powerful method for creating materials that are more difficult to synthesize by conventional processes. Application of the nanocasting technique in a fabrication process of mesoporous carbon materials implies as main novelty, the obtainment of a new nano-product inside of nanospaces provided by the pores of a porous solid (hard template). Structure replication on the nanometer length scale allows materials' properties to be manipulated in a controlled manner, such as tunable composition, controllable structure and morphology, and specific functionality. The nanocasting pathway with hard templates opens the door to the design of highly porous solids with multifunctional properties and interesting application perspectives.[4]

Basically, nanocasting comprises three steps: infiltration of the porosity of the template with a carbon precursor solution, heat treatment under a controlled atmosphere of template/carbon composite and removal of the template framework. Due to the fact that the synthesis takes place in the confined nanospaces, the sintering of the particles is restricted and the preparation of high surface area materials is achieved. In this way, numerous mesoporous carbons of high-surface area can be obtained, although high-temperatures are required to synthesize them. Moreover, this synthetic strategy clearly suggests that the structure of the synthesized carbon nanomaterials can be tailored depending on the pore characteristics of the selected template. The connectivity of the porous template directly affects the structure of the formed solid.

* Corresponding author: E-mail: mary_rud@yahoo.com; Tel: +40 232 201 135; Fax: +40 232 201 313

From the later periods, carbon materials have been synthesized using regularly structured template such as zeolite and mesoporous silica.[5-9] Preparation of ordered mesoporous carbons was widely demonstrated with different ordered mesoporous silica materials (MCM-48, SBA-15, SBA-1, and HMS) as template.[10-13] The first report by Ryoo's group on this pathway described the synthesis of mesoporous carbon with an ordered structure, where the replication of the MCM-48 structure led to the formation of a new type of mesoporous carbon material (CMK-1)[1]. Jun *et al.*[14] reported the first synthesis of a new type of mesoscopically ordered nanoporous (or mesoporous) carbon molecular sieve designated as CMK-3 by carbonizing sucrose inside the pores of the SBA-15 mesoporous silica molecular sieve.

In industrial applications, the activity per unit volume is more important than the activity per unit weight. The high microporosity, insufficient mechanical properties, and low density are probably the main reasons why porous carbons have not been applied industrially up to now.[15] In order to obtain a narrow pore size distribution and reduce the proportion of micropores, recently was developed a mesoporous carbon that exhibits well prospective properties, and which is of great potential for application as catalyst support.

As glycerol derived carbon displays very good structural and morphological properties, synthesis of microporous to mesoporous carbon using this carbon precursor has been carried out by using SBA-15 template instead to the carbon synthesis using sucrose as carbon source.

RESULTS AND DISCUSSION

Small and large-angle X-ray patterns of the SBA-15 silica template and obtained mesoporous carbon materials based on two different types of carbon precursors – sucrose, respective glycerol (CMs, CMg) – are presented in Fig. 1. As the carbon structure obtained by templating SBA-15 silica is a true replica of the one corresponding to the original silica,[14] three peaks, in the low angle XRD patterns, could be indexed as (100), (110), and (200) diffractions, which are associated with p6mm hexagonal symmetry indicating a retention of the ordered structure of its parent SBA-15 host.[16] There is an analogy between both structures, independent of the type of carbon precursor used in the synthesis of mesoporous carbon. The calculated cell parameters of the templated ordered mesoporous carbon materials are of 9.6 nm, and do not depend on the type of carbon precursor. In comparison with the silica template, the CMg and CMs carbons show cell parameters (9.6 nm), which are 15% lower than those of SBA-15 (11.3) (Table 1). This suggests that the silica suffer a structural shrinkage[17] that occurs in the replication process of SBA-15. This phenomenon is a consequence of the fact that obtained polymers undergo a substantial volume contraction during pyrolysis. Comparing the synthesized carbon samples, the sucrose derived carbon (CMs) is less well ordered and only exhibits the basal (100) peak.

The high angle XRD patterns of the CM samples exhibit peaks at $2\theta = 25°$ and 44° which can be respectively ascribed to (002) and (101) diffractions from the graphitic pore walls. The broadening of these peaks suggests the possible presence of an amorphous carbon phase.

The low magnification SEM images (Fig. 2) show that the mesoporous carbon materials are made up of rod particles. The carbon rods are rigidly interconnected by smaller carbon rods which are formed inside the micropores of main cylindrical pores of SBA-15. Sample CMg retained perfectly the rod-like morphology of the parent silica, whereas sample CMs retained the same morphology, but a lesser degree. This is consistent with the XRD and nitrogen sorption data.

Fig. 3 illustrates the nitrogen adsorption/ desorption isotherms and pore size distributions for the SBA-15 silica and templated mesoporous carbon CMg and CMs. The sharp step with a hysteresis loop for the isotherm of the host SBA-15 indicates a narrow pore size distribution and a uniform mesopore diameter of 7.6 nm. On the other hand, the CMs replica exhibits type IV nitrogen sorption isotherm with a well-developed capillary condensation step into mesopores in the range of 0.5 and 0.6 P/P_0, indicating a good mesostructural ordering. Sample CMg displays an isotherm that suggests the presence of micropores and/or small mesopores; the type H_4–hysteresis loop shows adsorption and desorption branches parallel to each other and almost horizontal.[18] The characteristics demonstrated above correspond to the materials having pores of slit-like shapes (commonly found for carbons).

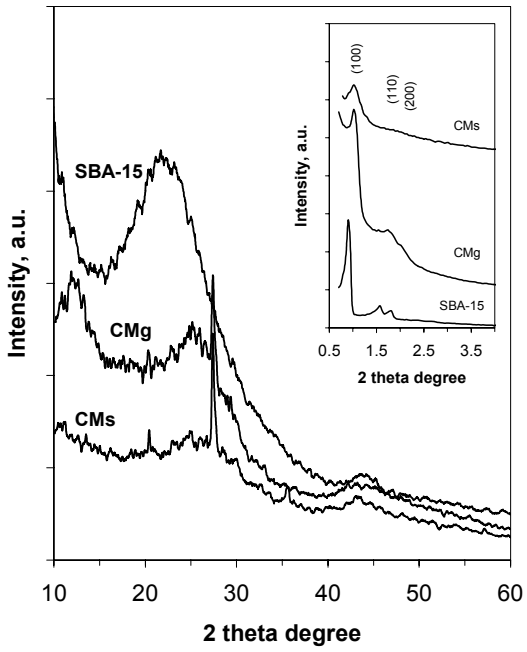

Fig. 1 – Powder X-ray diffraction patterns of SBA-15 silica and CMs and CMg mesoporous carbon.

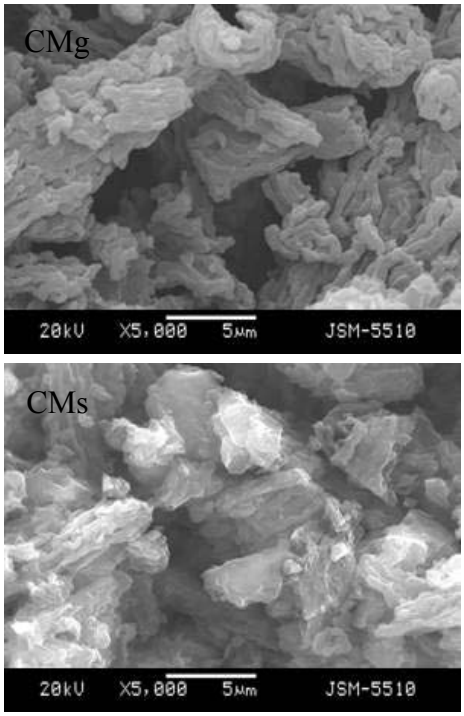

Fig. 2 – SEM images of rod-like mesoporous carbon materials CMg and CMs.

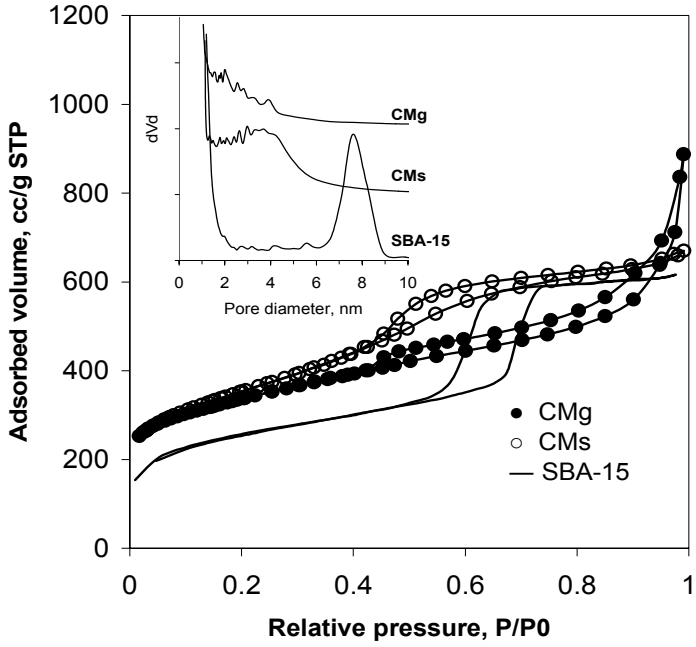

Fig. 3 – BET adsorption isotherms and corresponding PSDs of SBA-15 silica template and synthesized mesoporous carbon CMg and CMs.

The isotherms allow the calculation of a high BET surface area of 1258 m^2/g (CMs) and 1183 m^2/g (CMg), respectively for the templated carbons. The total pore volume is primarily related to the volume of the pores formed after silica dissolution. The hysteresis does not close at high relative pressure, because of the interparticle textural pores formed in the mesoporous carbon material.

Table 1

Textural and structural properties of SBA-15 silica template and synthesized mesoporous carbon based on carbonization process of glycerol and sucrose

Sample	Surface area, m^2/g	Pore volume, cc/g STP	Pore diameter, nm	α_s-plot results		d_{100}, nm	a_0, nm
				V_μ, cc/g STP	S_μ, m^2/g		
SBA-15	870	0.95	7.6	0.182	383	9.8	11.3
CMg	1183	0.99	< 3.7	0.194	437	8.3	9.6
CMs	1258	0.99	~ 3.7	0.125	292	8.3	9.6

Specific surface area calculation is based on the BET model; Total pore volume derived from the adsorption capacity; Mean mesopore diameter is calculated according to the BJH model using the adsorption branch; V_μ, S_μ = micropore volume and surface area derived from *t*-plot analysis; d_{100}, the d-spacing values were calculated by the formula $d_{100} = k/2\sin h$; a_0, unit cell parameter.

Fig. 3 (inset) indicates that the average pore size of the CMs carbon sample are ranging from 3 nm to 5 nm, while the pore size distribution of the CMg carbon sample shows a constant decrease in the range from 5 nm to 2 nm. The calculated pore size distribution data showed a pore size distribution centered at 7.5 nm for SBA-15 silica template. The expectedly large pore size is interesting when compared to the pore size of carbon samples. It is accepted because the smaller pore diameter in the case of carbons is due to the spaces that are forming during carbonization and silica removal processes. As observed, the variation of the pore size of mesoporous carbon depends on the modification of the structural parameters of the template during thermal treatment, and on the type of carbon sources used in the synthesis process. As result, there are differences in the micropore volume and surface area of the carbon samples. Therefore, the glycerol-based mesoporous carbon exhibit a higher micropore volume, respective a higher micropore surface area. The affirmation is proven also by the DFT calculations, being the main model characterizing slit-shaped pores (not shown here).

Fig. 4 shows the thermogravimetric analysis (TGA) of CMs and CMg carbon samples performed in oxygen atmosphere with a heating rate of 5 °C/min. The key information from the TG curves of carbons shown in the figure is that the silica template was not completely dissolved away by aqueous HF solution because of the less than 10% of residues after 600 °C for both carbon samples. The TG curves show a mass loss occurring in several steps, more clearly visible in the first derivative (DTG). It can be seen from the DTG curve that the sample CMg has one narrow peak centered at about 530 °C. A shoulder peak could be also observed meaning the oxidation process of carbon occurs in a complex way. On contrast, sample CMs displays two well-resolved weight loss events: one at the temperature of about 500 °C and the other one at about 535 °C, indicating the presence of two different carbon species as result of more complex decomposition process. With consideration of the data shown in Fig. 1, the carbon species showing a higher combustion temperature are attributed to the graphitic carbon, while the carbon species with a lower combustion temperature are ascribed to amorphous carbon.

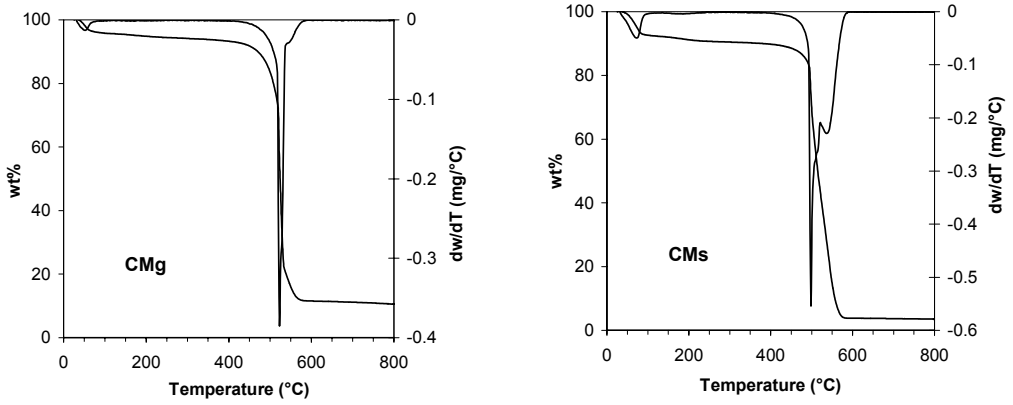

Fig. 4 – TGA and DTG of mesoporous carbon from (a) glycerol and (b) sucrose and SBA-15 material template.

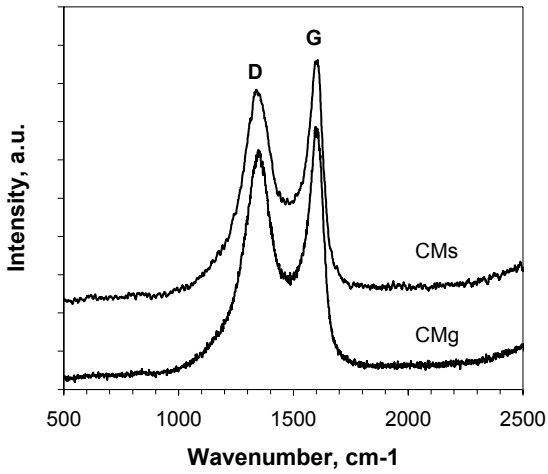

Fig. 5 – Raman spectra of mesoporous carbon materials.

The Raman spectra are consistent also with the XRD results and are shown in Fig. 5. As could be observed, the Raman spectra of the mesoporous carbon materials exhibit the presence of D and G bands, located at 1,342 and 1,599 cm^{-1} for CMg, and 1,339 and 1,600 cm^{-1} for CMs. The carbon samples synthesized in this work exhibit a very narrow G-band as compared with the other related mesoporous carbon materials. The peak at 1,599 cm^{-1}, 1,600 cm^{-1} respectively, corresponds to the Raman-active E_{2g}, which is due to the vibration mode corresponding to the movement in opposite directions of two neighboring carbon atoms in a single crystal graphite sheet. The D band at around 1,342 cm^{-1} (1,339 cm^{-1}) is associated with the presence of defects in the graphite layer. Furthermore, the relative intensity ratio of the D and G bands (I_D/I_G ratio) is proportional to the number of defect sites in the graphite carbon.[19,20] The I_D/I_G ratios are about 0.91 and 1.03 for the samples CMg and CMs, respectively, suggesting that the type of carbon precursor can improve the graphitic structure development. The I_D/I_G ratio can also be correlated with the degree of crystallinity, and as a result of this analysis the sample CMg appears to have a greater cristallinity than CMs.

EXPERIMENTAL

1. Synthesis SBA-15 mesoporous silica

SBA-15 was synthesized using the tri-block copolymer poly(ethylene glycol)-*block*-poly(propylene glycol)-*block*-poly(ethylene glycol) (Pluronic P123, Molecular weight = 5800, $EO_{20}PO_{70}EO_{20}$) (Aldrich) as a structure directing agent according to the method reported in the literature[21]. In a typical synthesis, 4 g of Pluronic P123 was added to 30 mL of water. After stirring for a few hours, a clear solution was obtained. Thereafter, 120 mL of 2 M HCl was added and the solution was stirred for another 2 h. Then, 9 g of tetraethylorthosilicate (Aldrich) was added and the resulting mixture was stirred for 24 h at 40 °C, and subsequently heated for 48 h to 100 °C. The solid product was recovered by filtration, washed several times with water, and dried overnight at 100 °C. Finally, the product was calcined at 550 °C to remove the template.

2. Synthesis of mesoporous carbon materials via nanocasting procedures

Mesoporous carbon was prepared by using SBA-15 silica as template and sucrose and glycerol (Aldrich) as the carbon sources. In a typical synthesis of mesoporous carbon, 1 g of template was added to a solution obtained by dissolving 1.25 g of sucrose and 0.08 mL of H_2SO_{4conc} in 4.5 ml of water, and keeping the mixture in an oven for 6 h at 100 °C. Subsequently, the oven temperature was raised to 160 °C for another 6 h. In order to obtain fully polymerized and carbonized sucrose inside the pores of the silica template, 0.75 g of sucrose, 0.05 ml of H_2SO_{4conc} and 5 ml of water were again added to the pretreated sample and the mixture was again subjected to the thermal treatment described above. The template-polymer composites were then pyrolyzed in a N_2 flow at 850 °C and kept under these conditions for 6 h to carbonize the polymer. The resulting SiO_2/C materials were then chemically treated with 9% HF solution overnight, in order to dissolve selectively the silica matrix leading to the ordered mesoporous carbon replicas. The same synthesis way was applied in the case of glycerol usage as carbon precursor.

3. Characterization

Powder X-ray Diffraction patterns (XRD) were collected with a Bruker D8 Advance X-ray instrument, using CuKα radiation (λ = 1.54184Å, Ni filter) in a θ:2θ configuration. Scanning electron Microscopy was performed by means of a SEM VEGA II LSH scanning electronic microscope manufactured by TESCAN for the Czech Republic, coupled with an EDX QUANTAX QX2 detector manufactured by ROENTEC Germany. N_2 adsorption-desorption isotherms at

-196 °C were performed on a Quantachrome Autosorb NOVA 2200 automated gas adsorption system. The isotherms were measured after outgassing of the samples under vacuum for 6 h at 200 °C. The Brunauer–Emmet–Teller (BET) method was used to calculate the specific surface area. The pore diameter was obtained using the Barret–Joyner–Halenda (BJH) method and the total pore volume was determined at $P/P_0 = 0.95$. Thermogravimetric measurements were performed on a Mettler TG50 thermobalance, equipped with an M3 microbalance and connected to a TC10A processor. Samples were heated from room temperature to 800 °C at a rate of 5 °C/min in an oxygen atmosphere. The Raman measurements were carried out using a Renishaw InVia micro-Raman spectrometer equipped with a charge coupled device (CCD). The Ar^+ laser (514.2 nm) with maximum power of 50 mW was used to excite the samples. Raman spectra were recorded in the 1000-3000 cm^{-1} region with 30 s integration times using a 50x objective culminating in a 3~5 cm^{-1} spectral resolution. Reported spectra use the cumulative result of 6 accumulations. All spectra were baseline corrected and deconvoluted using WIRE® software in order to strictly obtain the intensities and areas of the G and D bands to calculate their ratio.

CONCLUSIONS

In conclusion, ordered mesoporous carbons with rodlike structure were synthesized through the *in situ* conversion of the sucrose and glycerol to mesoporous carbon using mesoporous silica SBA-15 as template. Usage of glycerol results in a mesoporous carbon with mixed micro-meso pore structure; glycerol leads to formation of predominantly micropores with diameter around 2 nm, micropore volume of 0.194 cm^3gm^{-1}, and micropore surface area of 437 m^2/g. These textural results are of 1.5 times greater than that obtained in the case of the synthesis of mesoporous carbons obtained from sucrose. The glycerol-based mesoporous carbon exhibits a higher ordering and phase homogeneity as demonstrated by XRD and TGA measurements. These nanoporous carbon, having a highly graphitic framework, exhibits remarkably improved thermal stability, in comparison with sucrose-based mesoporous carbon. Due to the graphitic nature of the framework, the resultant mesoporous carbon would attract much attention for the development of new electrochemical applications, such as fuel cells and lithium ion batteries, as well as adsorption and catalysis fields. The edge-on graphitic structure exposed to pore's surface may also give interesting properties as a support for catalytic metal clusters.

Acknowledgments: The authors are grateful to Investigation Laboratory for the SEM measurements. S. Potgieter-Vermaak (*MiTAC*, UA) is acknowledged for the Raman measurements.

REFERENCES

1. R. Ryoo, S. H. Joo and S. Jun, *J. Phys., Chem. B*, **1999**, *103*, 7743-7746.
2. S. H. Joo, S. J. Choi, I. Oh, J. Kwak, Z. Liu, O. Terasaki and R. Ryoo, *Nature,* **2001**, *412*, 169.
3. J. Lee, S. Yoon, T. Hyeon, S.M. Oh and K.B. Kim, *Chem. Commun.,* **1999**, 2177.
4. A.-H. Lu and F. Schüth, *Adv. Mater.,* **2006**, *18*, 1793-1805.
5. N.Y.C. Yang, K. Jian, I. Kulaots, G.P. Crawford and R.H. Hurt, *J. Nanosci. Nanotech.,* **2003**, *3*, 386.
6. M. Inagaki, K. Kaneko and T. Nishizawa, *Carbon* **2004**, *42*, 1401.
7. A. Vinu and K. Ariga, *Chem. Lett*., **2005**, *34*, 674.
8. H. Yang and D. Zhao, *J. Mater. Chem.,* **2005**, *15*, 1217.
9. A. Vinu and M. Hartmann, *Catal. Today*, **2005**, *102*, 189.
10. R. Ryoo, S.H. Joo, M. Kruk and M. Jaroniec, *Adv. Mater.,* **2001**, *13*, 677-81.
11. F. Schuth, *Adv. Mater.,* **2003**, *42*, 3604-22.
12. J. Lee, S. Han and T. Hyeon, *J. Mater. Chem.,* **2004**, *14*, 478-86.
13. H. Yang and D. Zhao, *J. Mater. Chem.,* **2005**, *15*, 1217-31.
14. S. Jun, S.H. Jo, R. Ryoo, M. Kruk, M. Jaroniec, Z. Liu, T. Oshuna and O. Terasaki, *J. Am. Chem. Soc.,* **2000**, *122*, 10712.
15. L. Kaluza and M. Zdrail, *Carbon,* **2001**, *39*, 2023-2034.
16. Antonio B. Fuertes, *Micro. Meso. Mat.*, **2004**, *67*, 273-281.
17. A.B. Fuertes and D.M. Nevskaia, *Micro. Meso. Mater.,* **2003**, *62*, 177.
18. F. Rouquerol, J. Rouquerol and K. Sing, "Adsortion by powders and porous solids. Principles, methodology and application"*,* London. Academic Press, 1999.
19. V. Georgakilas, D. Voulgaris, E. Vazquez, M. Prato, D.M. Guldi, A. Kukovecz and H. Kuzmany, *J. Am. Chem. Soc.,* **2002**, *124*, 14318.
20. A.C. Ferrari and J. Robertson, *Phys. Rev. B,* **2000**, *61*, 14095.
21. M. Hartmann and A. Vinu, *Langmuir,* **2002**, *18*, 8010-8018.

ACADEMIA ROMÂNĂ
Revue Roumaine de Chimie
http://web.icf.ro/rrch/

Rev. Roum. Chim.,
2011, *56*(10-11), 947-952